

Phase Equilibria, Crystallization, and Microstructural Studies of the Flunixin Meglumine + Meglumine System

Songgu Wu,[†] Xiaobin Jiang,[†] Weibing Dong,[†] and Junbo Gong^{*,†}

[†]School of Chemical Engineering and Technology, Tianjin University, Tianjin 300072, People's Republic of China

^{*}Tianjin Key Laboratory of Modern Drug Delivery and High-Efficiency, Tianjin University, Tianjin 300072, People's Republic of China

ABSTRACT: The phase diagram of flunixin meglumine + meglumine system has been investigated with the method of differential scanning calorimetry (DSC). The results show that the flunixin meglumine and meglumine hold the formation of a simple eutectic mixture. The linear velocity of solidification of both pure components and the eutectic mixture was determined at different undercooling rates. The fusion enthalpy and the linear velocity of crystallization indicate the nonideal properties of the eutectic mixture in the melt. The roughness parameter of the eutectic system was calculated from the enthalpy of fusion value. The anisotropic and isotropic crystallizations of flunixin meglumine, meglumine, and the eutectic mixture were studied.

INTRODUCTION

Binary organic systems are ideal model systems for predicting solidification kinetics and microstructure control of physical properties due to the low transformation temperature, transparency, ease in purification, and wider choice of materials.^{1,2} Though the eutectic solidification seems to be simple and there have been considerable studies on the solidification behavior of organic eutectic systems, the mechanism of solidification kinetics, the nature of interactions and microstructures has yet not been fully explored.

It has been observed that the properties of composite materials depend on their microstructures. Anisotropic growth is one of the most efficient techniques in the domain of solidification phenomena.³

In the design and development of melt crystallization process, solid–liquid equilibrium (SLE) data are essential. Various methods had been proposed to measure the SLE, and the methods of using output data of differential scanning calorimetry (DSC) are suggested as an accurate means in recent years.⁴ This method is a sensitive and rapid technique, extensively used for determining the phase boundaries by measuring the heat effect during the phase transition.⁵ This study aims to measure the SLE data for binary systems containing the *N*-methyl-*D*-glucamine salt of flunixin (flunixin meglumine, FM, the IUPAC systematic name is (2*S*,3*R*,4*R*,5*R*)-2,3,4,5,6-pentahydroxy-*N*-methyl-1-hexanaminium 2-(2-methyl-3-(trifluoromethyl)anilino)nicotinate)) and meglumine (1-deoxy-1-(methylammonio)-*D*-glucitol) using the differential scanning calorimetry (DSC) technique. FM is a potent non-narcotic analgesic agent,⁶ and meglumine is one of main raw materials for the preparation of flunixin meglumine.

EXPERIMENTAL SECTION

Materials and Their Purification. Flunixin meglumine and meglumine (supplied by Zhejiang, Haixiang Pharmaceutical Co., Ltd., China) were purified by two times recrystallization from anhydrous ethanol, respectively (preparation of 333.1 K saturated solution of flunixin meglumine and meglumine, respectively, and then cooling them to 283.1 K with a rate of 0.0033 K·s⁻¹). The purified samples were analyzed by high-performance liquid chromatography (HPLC), and the mass fraction purity was

>0.99. Anhydrous ethanol (purchased from Tianjin Kewei Chemical Co., Ltd. of China) used was of analytical reagent (AR) grade, and the mass fraction purity was >0.997.

Equipment. The calorimetry experiments were performed on a NETZSCH DSC 204 differential scanning calorimeter equipped with sample and reference standard aluminum crucibles. During the scanning operation, nitrogen gas was purged through the DSC chamber at (0.667 to 0.833) mL·s⁻¹. The measurements were operated under a constant heating rate of 0.0167 K·s⁻¹. This scanning rate is low enough to approach the equilibrium measurement conditions. The temperature range is from (303.1 to 423.1) K (The cooling cycle was not taken into account. The reason is the viscosity of the melted liquid is high, so it is difficult to obtain crystal form spontaneously. It will undergo vitrification and become glass-like). Before the analysis, the energy flow was determined by calibration with the enthalpy of fusion of indium. The temperature was calibrated by a nominal platinum resistance thermometer. The uncertainties of the measurements were estimated to be ± 0.1 K for the temperature and ± 0.20 kJ·mol⁻¹ for the enthalpy of fusion.

Phase Diagram Studies. The phase diagram of the system was studied by DSC. Different amounts of flunixin meglumine and meglumine were accurately weighed (± 0.0001 g) in mortar, and the mixture was grinded for two hours to ensure homogeneous mixing. Then about (5 to 6) mg of solid was taken and sealed in a sample crucible for the analysis. As described in detail in the literature,⁷ we adopted the method in which liquid and solid curves were estimated from the onset and peak temperatures obtained from the measured DSC curves. Plotting the heat flow rate versus temperature, it shows that the onset temperature of DSC curves of the same sample based on the scanning rates of (0.0333 K·s⁻¹ and 0.0167 K·s⁻¹) are the same. The results show that the onset temperature is not affected by thermal history. The onset temperature at each first peak almost shows a constant value for the eutectic temperature. The next peak

Received: September 25, 2011

Accepted: November 1, 2011

Published: November 17, 2011

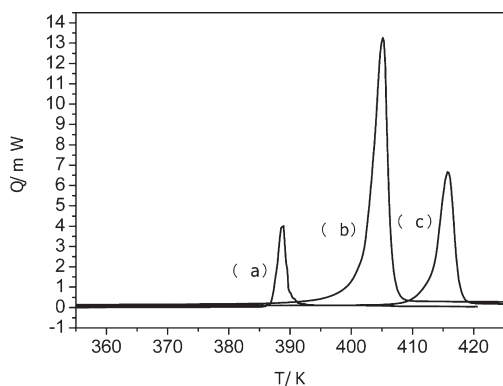


Figure 1. DSC curves for the flunixin meglumine + meglumine eutectic system. (a) Flunixin meglumine + meglumine eutectic, (b) meglumine, (c) flunixin meglumine.

Table 1. Thaw Melting Temperature (T_E) and Melting Temperature (T_{fus}) Values for Flunixin Meglumine + Meglumine

| x (mole fraction of meglumine) | T_E /K | T_{fus} /K |
|----------------------------------|-------------|--------------|
| 0.0000 | | 413.0 ± 0.1 |
| 0.0500 ± 0.0001 | 387.4 ± 0.1 | 411.0 ± 0.1 |
| 0.1500 ± 0.0001 | 387.3 ± 0.1 | 407.4 ± 0.1 |
| 0.2578 ± 0.0001 | 387.3 ± 0.1 | 402.9 ± 0.1 |
| 0.4991 ± 0.0001 | 387.4 ± 0.1 | 395.6 ± 0.1 |
| 0.5570 ± 0.0001 | 387.4 ± 0.1 | 391.6 ± 0.1 |
| 0.6020 ± 0.0001 | 387.4 ± 0.1 | 390.1 ± 0.1 |
| 0.6600 ± 0.0001 | 387.3 ± 0.1 | 387.3 ± 0.1 |
| 0.7001 ± 0.0001 | 387.2 ± 0.1 | 389.9 ± 0.1 |
| 0.7446 ± 0.0001 | 387.3 ± 0.1 | 392.3 ± 0.1 |
| 0.8710 ± 0.0001 | 387.2 ± 0.1 | 397.7 ± 0.1 |
| 0.8970 ± 0.0001 | 387.3 ± 0.1 | 398.8 ± 0.1 |
| 1.0000 | | 402.0 ± 0.1 |

temperatures are solidus temperatures. Figure 1 shows the representative DSC of flunixin meglumine, meglumine, and the eutectic mixture. The thaw points and melting points of different mixtures containing flunixin meglumine and their respective mean deviation are given in Table 1. These experimental points are shown in Figure 2 as a function of the mole fraction of meglumine.

Determination of Linear Velocity of Solidification. The linear velocities of crystallization of flunixin meglumine, meglumine, and their eutectic mixture at different undercooling temperatures were measured by the method described in detail previously.⁸ The measurements were made in heat-resistant glass tubes. The pure components and the eutectic mixture in the form of fine powders were filled separately in the glass tubes and placed in an oven maintained at a temperature slightly above their melting temperatures. After complete melting, the oven chamber was allowed to cool a few degrees below the melting temperatures of the samples. In each set of experiment performed, a seed crystal of the eutectic mixture and the pure component was separately added in the melt. On adding the seed, crystal nucleation and crystallization started linearly in the tube. The rate of solidification, determined from the movement of solid front as a function of time, was plotted against under-cooling (ΔT) using the Hillig–Turnbull equation.⁹

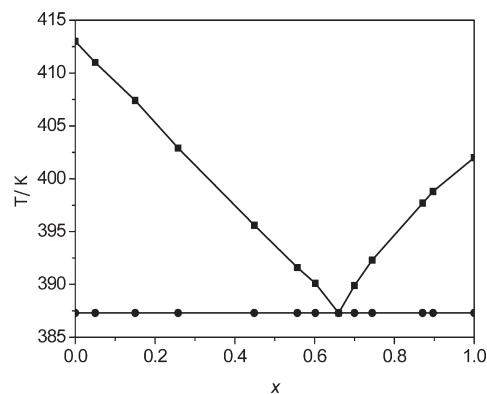


Figure 2. Phase diagram of the flunixin meglumine + meglumine eutectic system. ■, melting temperature; ●, thaw melting temperature; x is the mole fraction of meglumine.

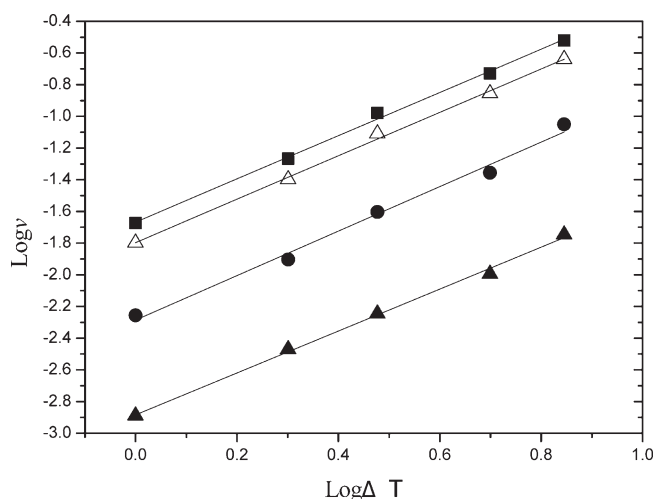


Figure 3. Linear velocity of solidification: ●, flunixin meglumine; ■, meglumine; ▲, eutectic (experimental); △, eutectic (mixture law).

Microstructure. Separate glass slides of flunixin meglumine, meglumine, and their eutectic mixture were prepared by placing a few fine powders on glass slides and then placing them in an oven maintained at a temperature slightly above their melting temperature. Both isotropic and anisotropic growth patterns of the samples were studied with the help of an optical microscope (Olympus U-CMAD3, Japan) at a suitable magnification.

RESULTS AND DISCUSSION

The phase diagrams of the flunixin meglumine and meglumine have been given in the form of temperature–composition curves (Figure 2). The phase diagram indicates the formation of a eutectic mixture at a (0.6600 ± 0.0001) mole fraction of meglumine which melts at (387.3 ± 0.1) K.

The relationship of linear velocity of crystallization (v) and undercooling (ΔT) is described by Hillig–Turnbull.⁹

$$v = k(\Delta T)^n \quad (1)$$

where k is the kinetic coefficient and n is a constant. Straight lines are obtained when $\log v$ is plotted against $\log (\Delta T)$ (Figure 3). From the slopes and intercepts of the straight lines, the values of n and k in each case were calculated. The experimental values of

Table 2. Crystallization Parameters and Enthalpy of Fusion Values for Flunixin Meglumine, Meglumine, and the Eutectic Mixture

| systems | k | | $\Delta_{\text{fus}}H$ kJ·mol ⁻¹ | $\Delta_{\text{fus}}S$ J·K ⁻¹ ·mol ⁻¹ | α | |
|---------------------------------|-------------------------------------|---------------|--|--|-------------|--------------|
| | mm·s ⁻¹ ·K ⁻¹ | n | | | $\xi = 0.5$ | $\xi = 1.0$ |
| flunixin meglumine | 0.0052 ± 0.0002 | 1.404 ± 0.003 | 64.03 ± 0.24 | 155.0 ± 0.8 | 9.30 ± 0.06 | 18.60 ± 0.12 |
| meglumine | 0.0215 ± 0.0004 | 1.363 ± 0.002 | 46.22 ± 0.25 | 114.7 ± 0.9 | 6.90 ± 0.05 | 13.80 ± 0.10 |
| eutectic mixture (experimental) | 0.0013 ± 0.0001 | 1.323 ± 0.005 | 43.68 ± 0.24 | 112.8 ± 0.7 | 6.78 ± 0.04 | 13.56 ± 0.08 |
| eutectic mixture (mixture law) | 0.0160 ± 0.0002 | 1.369 ± 0.049 | 52.27 ± 0.20 | 134.9 ± 0.7 | 8.1 ± 0.04 | 16.2 ± 0.08 |

the crystallization parameters, n and k , are given in Table 2, which rest with the solidification process of materials. A value of n less than 2 indicates slower variation in the growth velocity with undercooling, in comparison to the cases where n is equal to 2 which represents the square relationship between the growth velocity and the undercooling.

The linear velocity of crystallization (v) for the eutectic mixture was also calculated by using the mixture law (eq 2).

$$v_e = x_1 v_1 + x_2 v_2 \quad (2)$$

where x_1 and x_2 are the mole fractions of flunixin meglumine and meglumine, and v_e , v_1 , and v_2 are the linear velocities of crystallization of the eutectic mixture, flunixin meglumine, and meglumine, respectively. A straight line for the eutectic mixture is obtained when $\log v$ (as calculated from the mixture law) is plotted against $\log(\Delta T)$ (Figure 3). It is observed that the linear velocities of crystallization for the eutectic mixture at different undercoolings, calculated by the mixture law, are higher than the experimental values. This suggests the possibility of existence of some sort of molecular association or weak interaction between flunixin meglumine and meglumine. It is obvious that the linear velocity of crystallization increases as the undercooling temperature increases, and the experimental values of the linear velocities of crystallization of individual components are found to be higher than the linear velocities of crystallization of the eutectic mixture. This could be explained on the basis of the mechanism as proposed by Winegard et al.¹⁰ As reported in the literature, the crystal growth begins with the nucleation of the component which has a high melting temperature. The crystal grows continuously until the liquid of the other phase enrich around it. As a result of the concentration increasing, the second component then starts nucleating. When solidification of the eutectic is slower than that of the parent components, there is a possibility of alternate nucleation of the two components; therefore, in the case of the present eutectic system, the solidification mechanism follows an alternate nucleation of the two components. Therefore, the eutectic system cannot be considered as a simple mixture.¹¹

The fusion heats of the eutectic and pure components were determined by DSC. The results were shown in Table 2. The different thermal parameters, ΔH_{fus} , ΔS_{fus} , and Jackson's roughness parameter (α) have been determined with the experimental data. The DSC curves of flunixin meglumine, meglumine, and the eutectic mixture are shown in Figure 3. The enthalpy of fusion values of the eutectic mixture can be calculated by using a mixture law (eq 3).

$$(\Delta_{\text{fus}}H)_e = (x_1)_e(\Delta_{\text{fus}}H)_1 + (x_2)_e(\Delta_{\text{fus}}H)_2 \quad (3)$$

where $(\Delta H_{\text{fus}})_1$ and $(\Delta H_{\text{fus}})_2$ are the fusion enthalpies of components 1 and 2, respectively. The fusion enthalpy as calculated from the mixture law (52.27 ± 0.20 kJ·mol⁻¹) is higher than the

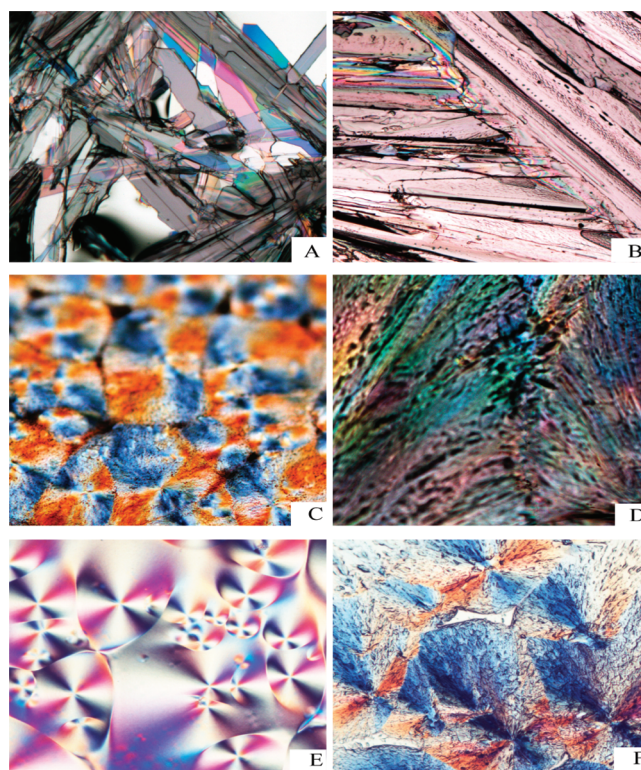


Figure 4. Microstructures for flunixin meglumine + meglumine eutectic system. (A) Flunixin meglumine anisotropic, (B) flunixin meglumine isotropic, (C) meglumine anisotropic, (D) meglumine isotropic, (E) flunixin meglumine + meglumine eutectic anisotropic, (F) flunixin meglumine + meglumine eutectic isotropic.

experimentally determined value (48.68 ± 0.24 kJ·mol⁻¹). It indicates the existence of some interactions between the two phases, namely, flunixin meglumine and meglumine.

The values of entropy of fusion of the pure components and the eutectic were calculated as follows.¹²

$$(\Delta_{\text{fus}}S) = (\Delta_{\text{fus}}H)/T_{\text{fus}} \quad (4)$$

where T is the fusion temperature. The values of entropy of fusion have been given in Table 2. As ΔS_{fus} values are positive, indicating that the entropy factor favors the solidification process. It is clear that the entropy factor is more effective in the melting process to pure components than to the eutectic.

According to Hunt and Jackson, the type of growth from a eutectic melt depends upon a factor α , defined as,¹³

$$\alpha = \xi(\Delta_{\text{fus}}S)/R = \xi(\Delta_{\text{fus}}H)/RT_{\text{fus}} \quad (5)$$

where ξ is the geometrical coefficient whose value lies between 0.5 and 1.0. The values of α for the eutectic mixture and the two

pure components were calculated by putting the ξ value equal to 0.5 and 1.0, respectively. The value of Jackson's roughness parameter greater than 2 suggests that the faceted growth in all of the systems. The solid–liquid interface is atomically smooth and advances into the liquid by the propagation of atomic steps across the interface. This means the process requires a considerable undercooling degree.

The optical microphotographs of the flunixin meglumine, meglumine, and their eutectic have been given in Figure 4A–F. Various physical properties of materials rest on their crystallization behavior and microstructures. The anisotropic crystallization pattern of flunixin meglumine appears like the thin sheets stacked together (Figure 4A), whereas meglumine crystallized anisotropically gives a beautiful floral structure (Figure 4C). However, in the case of the eutectic mixture, a spherulitic-type structure (Figure 4E) is obtained. It is noticed that the microstructure obtained on isotropic crystallization is completely different from the anisotropic ones. The isotropic microstructure of flunixin meglumine shows a palm leaf type structure (Figure 4B). Meglumine crystallized isotropically gives a lamellar-type structure with thin lamellae (Figure 4D). The isotropic crystallization pattern of the eutectic mixture looks like a butterfly (Figure 4F). These microstructures show that the crystallization of the eutectics have different characteristics from the parent components. As the formation of the eutectic microstructures depends on various factors, such as the properties and molecular structure of the components, interface contact angles, concentration gradient, diffusion, nucleation, and crystallization characteristics of the pure components and type of defects present in the growing nuclei,¹⁴ it is difficult to predict the microstructure of the eutectic accurately.

CONCLUSION

Phase diagram studies have shown that for flunixin meglumine and meglumine formation a eutectic mixture at (0.6600 ± 0.0001) mole fraction of meglumine was formed which melts at (387.3 ± 0.1) K. Linear velocities of crystallization and enthalpy of fusion values have suggested that the eutectic is a nonideal mixture. According to the roughness parameters, it is predicted that the eutectic mixture possesses a faceted morphology with an irregular structure.

AUTHOR INFORMATION

Corresponding Author

*Fax: +86-22-27374971. E-mail: junbo_gong@tju.edu.cn.

Funding Sources

This material is based upon work supported by National Natural Science Foundation of China (Nos. 20836005 and 21176173) and Tianjin Municipal Natural Science Foundation (Nos. 10JCYBJC14200 and 09JCZDJC20100). The analysis tools used in this study were supported by State Key Laboratory of Chemical Engineering (No. SKL-ChE-11B02).

REFERENCES

- (1) Gupta, R. K.; Singh, R. A. Thermochemical and Microstructural Studies on Binary Organic Eutectics and Complexes. *J. Cryst. Growth* **2004**, *26*, 340–347.
- (2) Agrawal, T.; Gupta, P.; Das, S. S. Phase Equilibria, Crystallization, and Microstructural Studies of Naphthalen-2-ol + 1,3-Dinitrobenzene. *J. Chem. Eng. Data* **2010**, *55*, 4206–4210.

- (3) Singh, N. B.; Agrawal, T.; Gupta, P.; Das, S. S. Solidification Behavior of the Benzamid + *O*-Chlorobenzoic Acid Eutectic System. *J. Chem. Eng. Data* **2009**, *54*, 1529–1536.

- (4) Ji, H. Z.; Meng, X. C.; Zhao, H. K. (Solid + Liquid) Equilibrium of (4-Chloro-2-benzofuran-1,3-dione + 5-Chloro-2-benzofuran-1,3-dione). *J. Chem. Eng. Data* **2010**, *55*, 2590–2593.

- (5) Hammami, A.; Mehrotra, A. K. Non-isothermal Crystallization Kinetics of *n*-paraffins with Chain Lengths Between Thirty and Fifty. *Thermochim. Acta* **1992**, *211*, 137–153.

- (6) Ciofalo, V. B.; Latranyi, M. B.; Patel, J. B. Flunixin Meglumine: a Non-narcotic Analgesic. *J. Pharmacol. Exp. Ther.* **1997**, *200*, 501–507.

- (7) Takiyama, H.; Suzuki, H.; Uchida, H.; Matsuoka, M. Determination of Solid-liquid Phase Equilibria by Using Measured DSC Curves. *Fluid Phase Equilib.* **2010**, *194–197*, 103–107.

- (8) Rastogi, R. P.; Bassi, P. S. Mechanism on Eutectic Crystallization. *J. Phys. Chem.* **1964**, *68*, 2398–2408.

- (9) Hillig, W. B.; Turnbull, D. Theory of Crystal Growth in Undercooled Pure Liquids. *J. Chem. Phys.* **1956**, *24*, 914–920.

- (10) Winegard, W. C.; Majka, S.; Thall, B. M.; Chalmers, B. Eutectic Solidification in Metals. *Can. J. Chem.* **1954**, *29*, 320–327.

- (11) Sharma, B. L.; Kant, R.; Sharma, R.; Tondon, S. Deviations of Binary Organic Eutectic Melts Systems. *Mater. Chem. Phys.* **2003**, *82*, 216–224.

- (12) Rai, U. S.; Mandal, K. D. Chemistry of Organic Eutectics: ρ -Phenylenediamine-*m*-Nitrobenzoic Acid System Involving the 1:2 Addition Compound. *Bull. Chem. Soc. Jpn.* **1990**, *63*, 1496.

- (13) Hunt, J. D.; Jackson, K. A. Lamellar and Rod Eutectic Growth. *Trans. Metall. Soc. AIME* **1966**, *236*, 1129–1142.

- (14) Das, S. S.; Singh, N. P.; Agrawal, T.; Gupta, P.; Tiwari, S. N.; Singh, N. B. Studies of Solidification Behavior and Molecular Interaction in Benzoic Acid-*o*-Chloro Benzoic Acid Eutectic System. *Mol. Cryst. Liq. Cryst.* **2009**, *501* (1), 107–124.